Supporting Information for

3D Lamellar-Structured Graphene Aerogels for Thermal Interface Composites with High Through-Plane Thermal Conductivity and Fracture Toughness

Pengfei Liu[1, 2], Xiaofeng Li[1,*], Peng Min[1], Xiyuan Chang[2], Chao Shu[1], Yun Ding[1], Zhong-Zhen Yu[2, 3,*]

[1] Beijing Key Laboratory of Advanced Functional Polymer Composites, Beijing University of Chemical Technology, Beijing 100029, China

[2] State Key Laboratory of Organic-Inorganic Composites, College of Materials Science and Engineering, Beijing University of Chemical Technology, Beijing 100029, China

[3] Beijing Advanced Innovation Center for Soft Matter Science and Engineering, Beijing University of Chemical Technology, Beijing 100029, China

*Corresponding authors. E-mail: xfli@mail.buct.edu.cn (X. Li); yuzz@mail.buct.edu.cn (Z.-Z. Yu)

Supplementary Figures and Tables

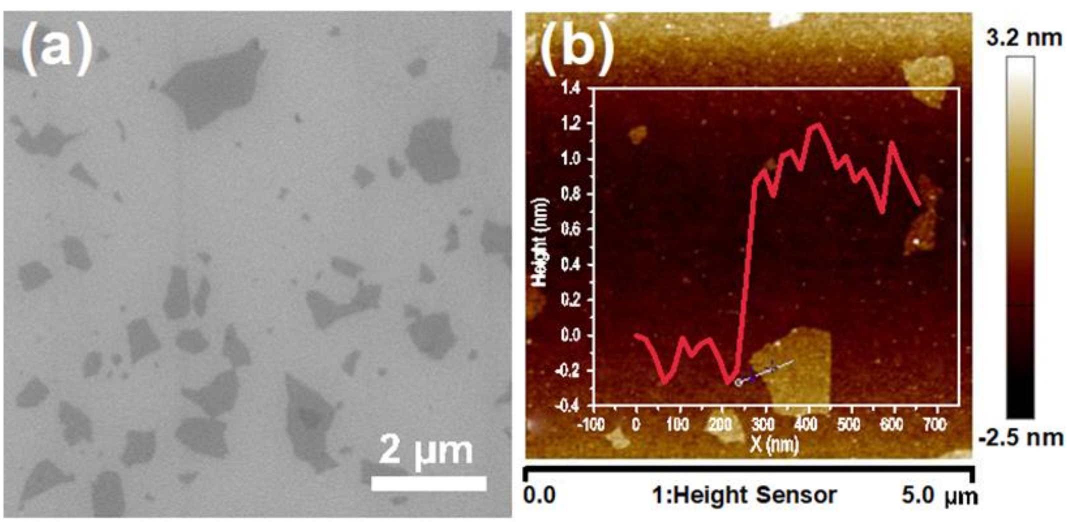

Fig. S1. (a) SEM image and (b) AFM image of GO sheets.

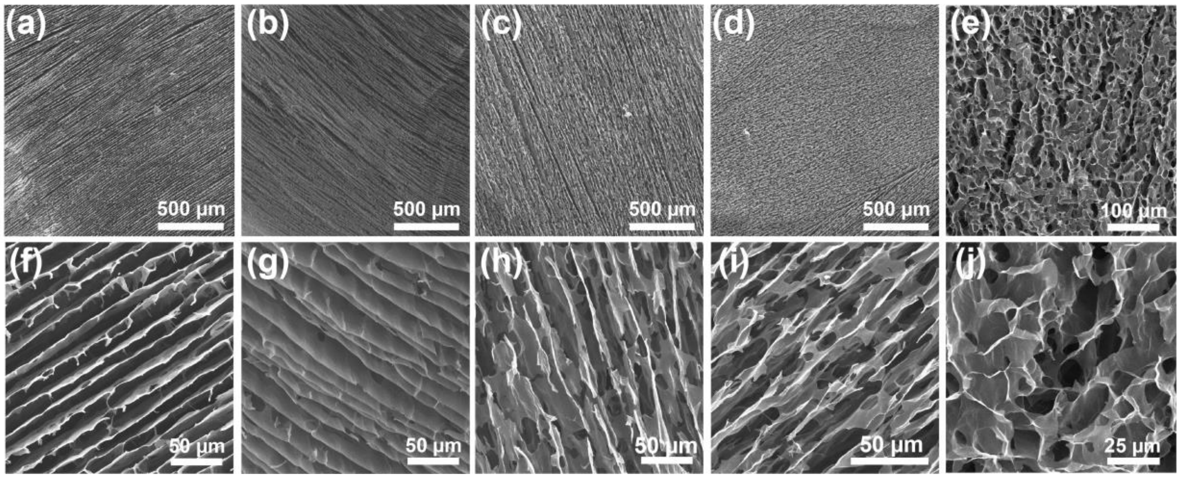

Fig. S2. (**a-e**) Low- and (**f-j**) high-magnification SEM images of morphologies of (**a, f**) P6G4, (**b, g**) P5G5, (**c, h**) P4G6, (**d, i**) P3G7, and (**e, j**) GO observed along Z-axis

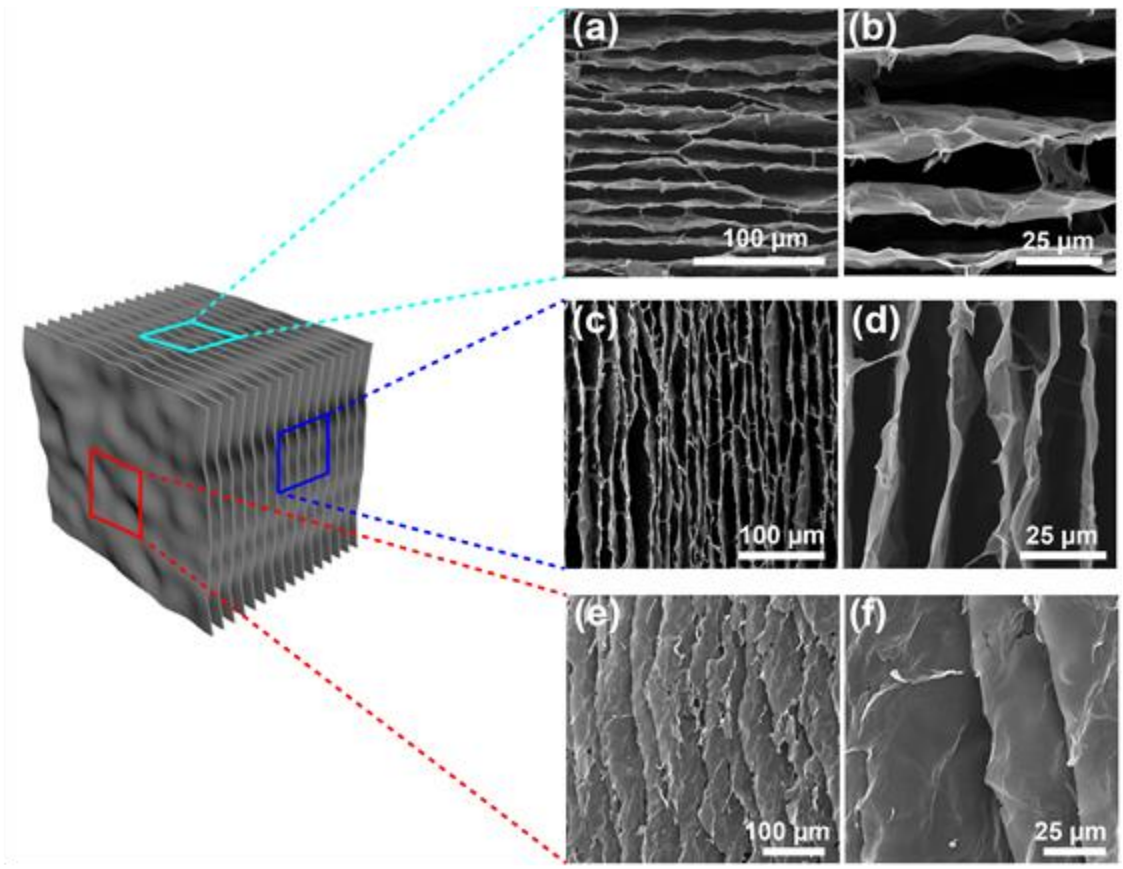

Fig. S3. SEM images of morphologies of P6G4-2800 observed along (**a, b**) Z-axis, (**c, d**) X axis, and (e, f) Y axis

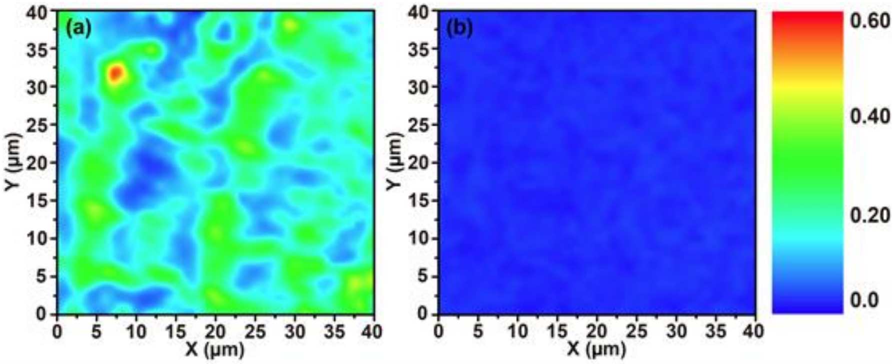

Fig. S4. Raman mapping images of (**a**) PAA-2800, and (**b**) GO-2800

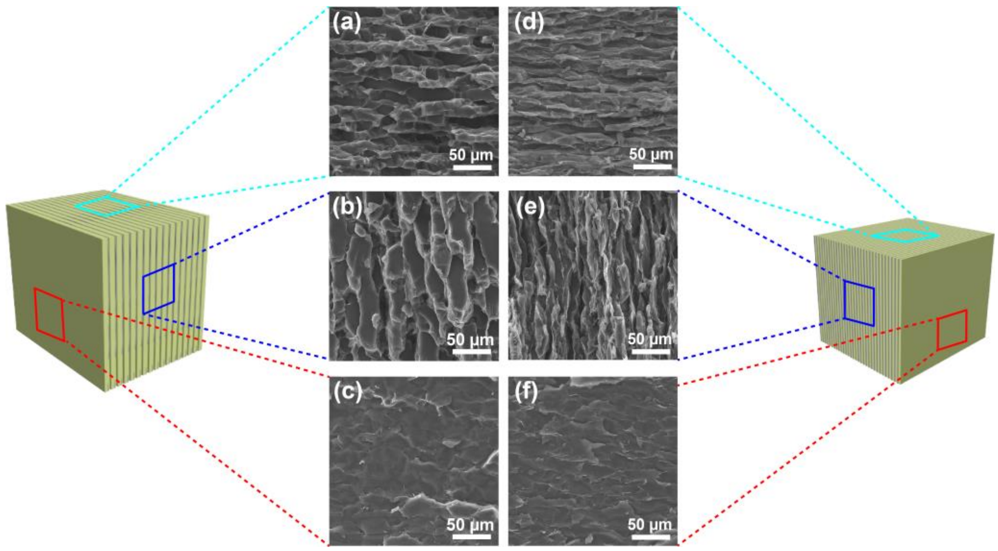

Fig. S5. SEM images of morphologies of (**a-c**) GE4 and (**d-f**) GE4-70% observed from three directions

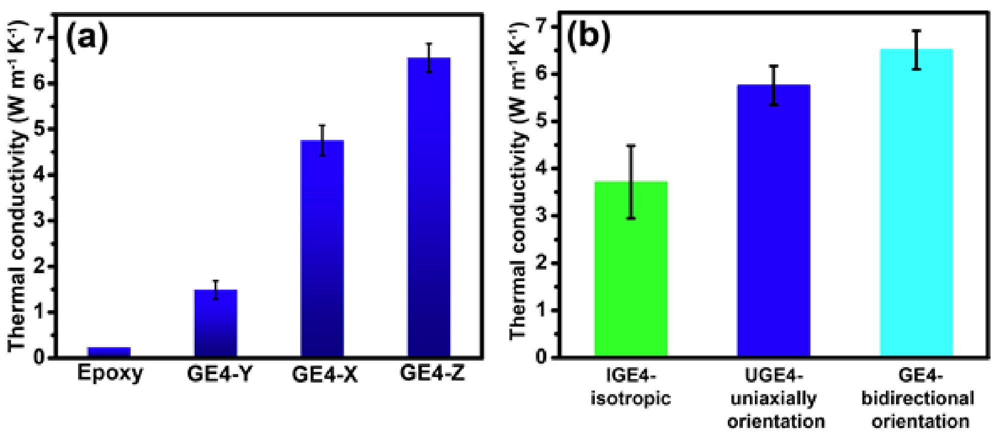

Fig. S6. (**a**) Comparison of thermal conductivities of GE4 in three directions. (**b**) Comparison of thermal conductivities of composites with isotropic aerogel (IGE4), and unidirectionally and bidirectionally orientated aerogels

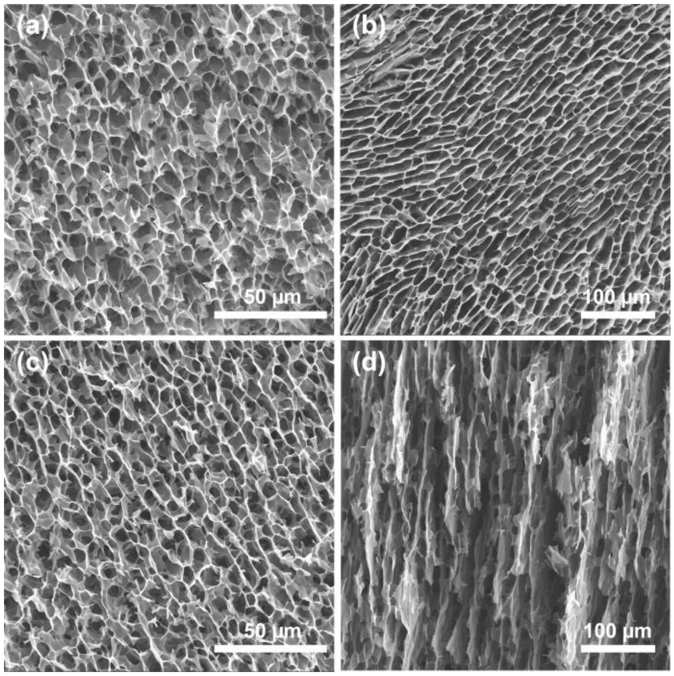

Fig. S7. Longitudinal view SEM images of (**a**) IP6G4-2800 and (**b**) UP6G4-2800. Transversal view SEM images of (**c**) IP6G4-2800 and (**d**) UP6G4-2800

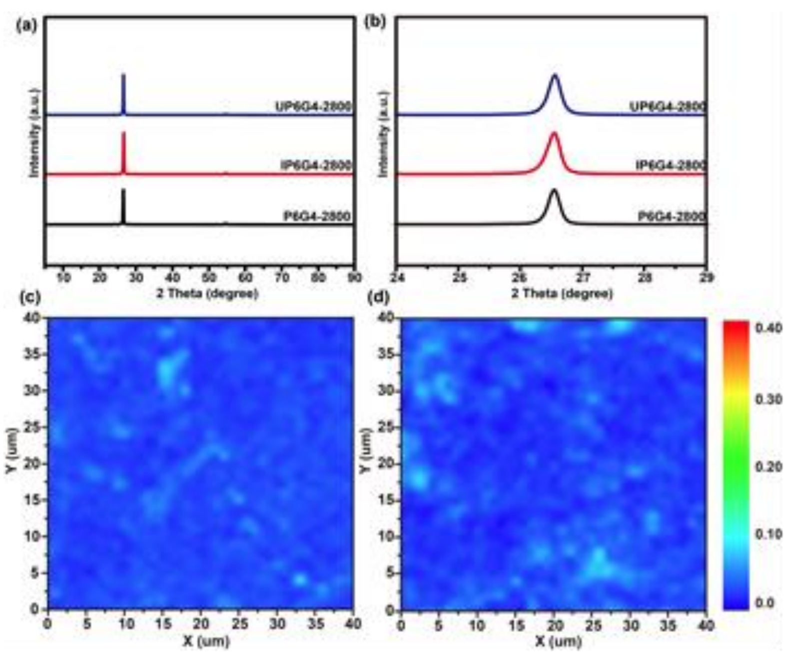

Fig. S8. (**a, b**) XRD patterns of P6G4-2800, IP6G4-2800 and UP6G4-2800. Raman mapping of (**c**) IP6G4-2800 and (**d**) UP6G4-2800. The average I_D/I_G of IP6G4-2800 and UP6G4-2800 are ~0.030 and ~0.031, respectively

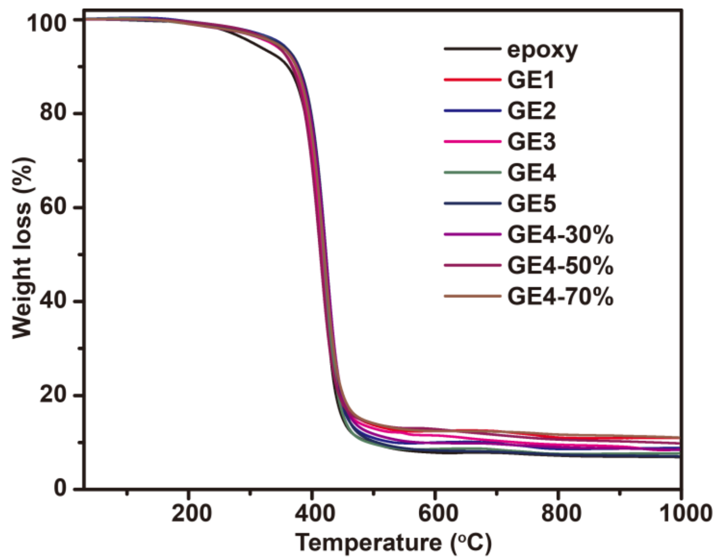

Fig. S9. TGA curves of epoxy and epoxy/LSGA composites

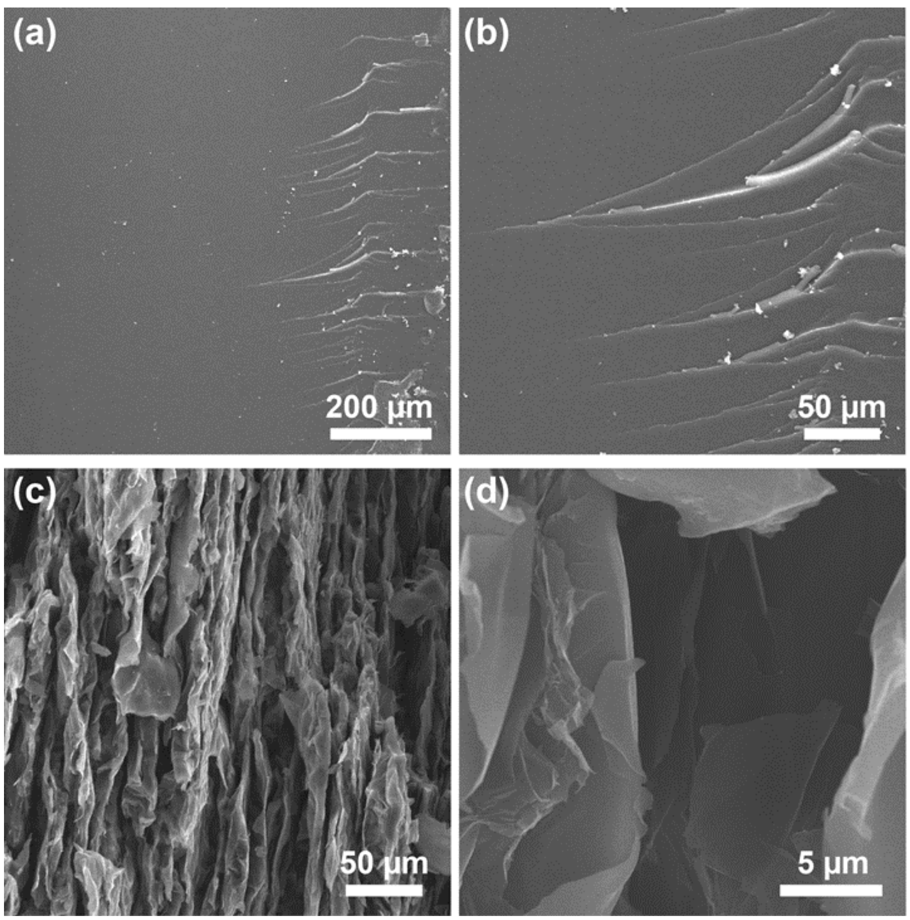

Fig. S10. Fracture surfaces of (**a, b**) epoxy and (**c, d**) GE4-70%

Table S1. Detailed ingredients of PAAS/GO hybrid aerogels

Aerogels	PAA (g)	TEA (g)	GO (g)	Water (g)
PAA	1.60	0.77	0	37.63
P9G1	1.44	0.69	0.16	37.71
P8G2	1.28	0.61	0.32	37.79
P7G3	1.12	0.54	0.48	37.86
P6G4	0.96	0.46	0.64	37.94
P5G5	0.80	0.38	0.80	38.02
P4G6	0.64	0.31	0.96	38.09
P3G7	0.48	0.23	1.12	38.17
GO	0	0	1.60	38.40

Table S2. Filler contents, through-plane thermal conductivities of graphene/epoxy composites, and average I_D/I_G values of LSGAs

Composites	Filler content (wt%)	Filler content (vol%)	Average I_D/I_G of LSGAs	Thermal conductivity in direction Z (W m^{-1} K^{-1})
GE1	4.42	2.39	0.087	6.20 ±0.20
GE2	2.29	1.22	0.072	6.53 ±0.33
GE3	1.60	0.86	0.044	6.07 ±0.38
GE4	1.23	0.68	0.036	6.51 ±0.41
GE5	0.99	0.53	0.028	5.57 ±0.30
GE4-30%	1.65	0.88	0.036	7.66 ±0.69
GE4-50%	2.7	1.45	0.036	12.77 ±0.90
GE4-70%	4.28	2.30	0.036	20.03 ±1.11

Table S3. Comparison of thermal conductivities and specific TCE of our composites with those reported in the literature

Fillers	Matrix	Content (vol%)	$K_{//}$= in-plane $K_{\perp}$= through-plane (W m^{-1} K^{-1})	Specific TCE	Ref.
RGO	Epoxy	~0.53	1.4	~1132	[1]
GNP	Epoxy	2.80	1.5	~244	[2]
GNP	Epoxy	~5.57	1.53	~119	[3]
GNP/CNT	Epoxy	~6.22	1.75	~125	[4]
3D graphene aerogel	Epoxy	0.92	$K_{\perp}$= 2.13	~1332	[5]
3D BNNS network	Epoxy	~9.29	$K_{\perp}$= 2.85	~181	[6]
Graphene	SBR	15.0	2.92	~90	[7]
GNP	Octadecanol	~3.83	3.55	~395	[8]
3D graphene foam	Wax	1.23	3.6	~1500	[9]
Graphene woven fabrics	PI	~7.79	$K_{//}$=3.73, $K_{\perp}$= 0.41	~182	[10]
3D BNNS network	Epoxy	34.0	$K_{\perp}$= 4.42	~66	[11]
3D graphene aerogel	Octadecanol	~1.58	4.28	~1065	[12]
3D BN-RGO network	Epoxy	13.16	$K_{\perp}$= 5.05	~206	[13]
Graphene	Epoxy	10.0	5.1	~230	[14]
RGO/GNP aerogel	Octadecanol	~4.67	5.92	~541	[15]
Aligned BN aerogel	Epoxy	15.0	$K_{\perp}$= 6.07	~196	[16]
GNP/CNT	Epoxy	50.0	7.3	~71	[17]
Aligned graphene aerogel	Wax	~1.31	$K_{//}$=2.68, $K_{\perp}$= 8.87	~1858	[18]
Graphene flakes	PVDF	25.0	$K_{//}$=10.19	~196	[19]
Graphene foam/ Graphene sheets	NR	6.20	$K_{//}$=10.64, $K_{\perp}$= 3.0	~1300	[20]
GNP	Epoxy	25.0	12.4	~282	[21]
3D graphene aerogel	PDMS	~5.34	$K_{//}$=28.77, $K_{\perp}$= 1.62	~2974	[22]
GNP	Epoxy	~6.60	$K_{//}$=33.54	~2526	[23]
Aligned graphene aerogel	Epoxy	19.0	$K_{//}$=17.1, $K_{\perp}$= 35.5	~884	[24]
Worm-like expanded graphite	Wax	~16.0	$K_{//}$=40	~1243	[25]
BNNS	Aramid nanofiber	~21.5	$K_{//}$=46.7, $K_{\perp}$= 0.13	~266	[26]
Aligned graphene aerogel	**Epoxy**	**2.30**	**$K_{\perp}$= 20.0**	**4310**	**This work**

Supplementary References:

[S1] O. Eksik, S.F. Bartolucci, T. Gupta, H. Fard, T. Borca-Tasciuc et al., A novel approach to enhance the thermal conductivity of epoxy nanocomposites using graphene core–shell additives. Carbon **101**, 239-244 (2016). https://doi:10.1016/j.carbon.2016.01.095

[S2] X. Shen, Z. Wang, Y. Wu, X. Liu, Y.B. He et al., Multilayer graphene enables higher efficiency in improving thermal conductivities of graphene/epoxy composites. Nano Lett. **16**(6), 3585-3593 (2016). https://doi:10.1021/acs.nanolett.6b00722

[S3] S.H. Song, K.H. Park, B.H. Kim, Y.W. Choi, G.H. Jun et al., Enhanced thermal conductivity of epoxy-graphene composites by using non-oxidized graphene flakes with non-covalent functionalization. Adv. Mater. **25**(5), 732-737 (2013). https://doi:10.1002/adma.201202736

[S4] A. Yu, P. Ramesh, X. Sun, E. Bekyarova, M.E. Itkis, R.C. Haddon, Enhanced thermal conductivity in a hybrid graphite nanoplatelet–carbon nanotube filler for epoxy composites. Adv. Mater. **20**(24), 4740-4744 (2008). https://doi:10.1002/adma.200800401

[S5] G. Lian, C.-C. Tuan, L. Li, S. Jiao, Q. Wang et al., Vertically aligned and interconnected graphene networks for high thermal conductivity of epoxy composites with ultralow loading. Chem. Mater. **28**(17), 6096-6104 (2016). https://doi:10.1021/acs.chemmater.6b01595

[S6] X. Zeng, Y. Yao, Z. Gong, F. Wang, R. Sun et al., Ice-templated assembly strategy to construct 3D boron nitride nanosheet networks in polymer composites for thermal conductivity improvement. Small **11**(46), 6205-6213 (2015). https://doi:10.1002/smll.201502173

[S7] Y. Li, F. Xu, Z. Lin, X. Sun, Q. Peng et al., Electrically and thermally conductive underwater acoustically absorptive graphene/rubber nanocomposites for multifunctional applications. Nanoscale **9**(38), 14476-14485 (2017). https://doi:10.1039/c7nr05189a

[S8] G. Xin, H. Sun, S.M. Scott, T. Yao, F. Lu, et al., Advanced phase change composite by thermally annealed defect-free graphene for thermal energy storage. ACS Appl. Mater. Interfaces **6**(17), 15262-15271 (2014). https://doi:10.1021/am503619a

[S9] H. Ji, D.P. Sellan, M.T. Pettes, X. Kong, J. Ji et al., Enhanced thermal conductivity of phase change materials with ultrathin-graphite foams for thermal energy storage. Energy Environ. Sci. **7**(3), 1185-1192 (2014). https://doi:10.1039/c3ee42573h

[S10] J. Gong, Z. Liu, J. Yu, D. Dai, W. Dai et al., Graphene woven fabric-reinforced polyimide films with enhanced and anisotropic thermal conductivity. Compos. A Appl. Sci. Manuf. **87**, 290-296 (2016). https://doi:10.1016/j.compositesa.2016.05.010

[S11] J. Hu, Y. Huang, Y. Yao, G. Pan, J. Sun et al., Polymer composite with improved thermal conductivity by constructing a hierarchically ordered three-dimensional interconnected network of BN. ACS Appl. Mater. Interfaces **9**(15), 13544-13553 (2017).

https://doi:10.1021/acsami.7b02410

[S12] J. Yang, X. Li, S. Han, R. Yang, P. Min et al., High-quality graphene aerogels for thermally conductive phase change composites with excellent shape stability. J. Mater. Chem. A **6**(14), 5880-5886 (2018). https://doi:10.1039/c8ta00078f

[S13] Y. Yao, J. Sun, X. Zeng, R. Sun, J.B. Xu et al., Construction of 3D skeleton for polymer composites achieving a high thermal conductivity. Small **14**(13), 1704044 (2018). https://doi:10.1002/smll.201704044

[S14] K.M. Shahil, A.A. Balandin, Graphene-multilayer graphene nanocomposites as highly efficient thermal interface materials. Nano Lett. **12**(2), 861-867 (2012). https://doi:10.1021/nl203906r

[S15] J. Yang, X. Li, S. Han, Y. Zhang, P. Min et al., Air-dried, high-density graphene hybrid aerogels for phase change composites with exceptional thermal conductivity and shape stability. J. Mater. Chem. A **4**(46), 18067-18074 (2016). https://doi:10.1039/c6ta07869a

[S16] J. Han, G. Du, W. Gao, H. Bai, An anisotropically high thermal conductive boron nitride/epoxy composite based on nacre-mimetic 3D network. Adv. Funct. Mater. **29**(13), 1900412 (2019). https://doi:10.1002/adfm.201900412

[S17] X. Huang, C. Zhi, P. Jiang, Toward effective synergetic effects from graphene nanoplatelets and carbon nanotubes on thermal conductivity of ultrahigh volume fraction nanocarbon epoxy composites. J. Phys. Chem. C **116**(44), 23812-23820 (2012). https://doi:10.1021/jp308556r

[S18] P. Min, J. Liu, X. Li, F. An, P. Liu et al., Thermally conductive phase change composites featuring anisotropic graphene aerogels for real-time and fast-charging solar-thermal energy conversion. Adv. Funct. Mater. **28**(51), 1805365 (2018). https://doi:10.1002/adfm.201805365

[S19] H. Jung, S. Yu, N.S. Bae, S.M. Cho, R.H. Kim et al., High through-plane thermal conduction of graphene nanoflake filled polymer composites melt-processed in an l-shape kinked tube. ACS Appl. Mater. Interfaces **7**(28), 15256-15262 (2015). https://doi:10.1021/acsami.5b02681

[S20] Z. Wu, C. Xu, C. Ma, Z. Liu, H.M. Cheng et al., Synergistic effect of aligned graphene nanosheets in graphene foam for high-performance thermally conductive composites. Adv. Mater. **31**(19), 1900199 (2019). https://doi:10.1002/adma.201900199

[S21] M. Shtein, R. Nadiv, M. Buzaglo, K. Kahil, O. Regev, Thermally conductive graphene-polymer composites: size, percolation, and synergy effects. Chem. Mater. **27**(6), 2100-2106 (2015). https://doi:10.1021/cm504550e

[S22] H. Fang, Y. Zhao, Y. Zhang, Y. Ren, S.L. Bai, Three-dimensional graphene foam-filled elastomer composites with high thermal and mechanical properties. ACS Appl. Mater. Interfaces **9**(31), 26447-26459 (2017). https://doi:10.1021/acsami.7b07650

[S23] Q. Li, Y. Guo, W. Li, S. Qiu, C. Zhu et al., Ultrahigh thermal conductivity of assembled aligned multilayer graphene/epoxy composite. Chem. Mater. **26**(15), 4459-4465 (2014). https://doi:10.1021/cm501473t

[S24] F. An, X. Li, P. Min, P. Liu, Z.G. Jiang et al., Vertically aligned high-quality graphene foams for anisotropically conductive polymer composites with ultrahigh through-plane thermal conductivities. ACS Appl. Mater. Interfaces **10**(20), 17383-17392 (2018). https://doi:10.1021/acsami.8b04230

[S25] S. Wu, T. Li, Z. Tong, J. Chao, T. Zhai et al., High-performance thermally conductive phase change Ccomposites by large-size oriented graphite sheets for scalable thermal energy harvesting. Adv. Mater. **31**(49), 1905099 (2019). https://doi:10.1002/adma.201905099

[S26] K. Wu, J. Wang, D. Liu, C. Lei, D. Liu et al., Highly thermoconductive, thermostable, and super-flexible film by engineering 1D rigid rod-like aramid nanofiber/2D boron nitride nanosheets. Adv. Mater. **32**(8) 1906939 (2020). https://doi:10.1002/adma.201906939